Cell Reports, Volume *36*

Supplemental information

Exocyst protein subnetworks integrate Hippo and mTOR signaling to promote virus detection and cancer

Aubhishek Zaman, Xiaofeng Wu, Andrew Lemoff, Sivaramakrishna Yadavalli, Jeon Lee, Chensu Wang, Jonathan Cooper, Elizabeth A. McMillan, Charles Yeaman, Hamid Mirzaei, Michael A. White, and Trever G. Bivona

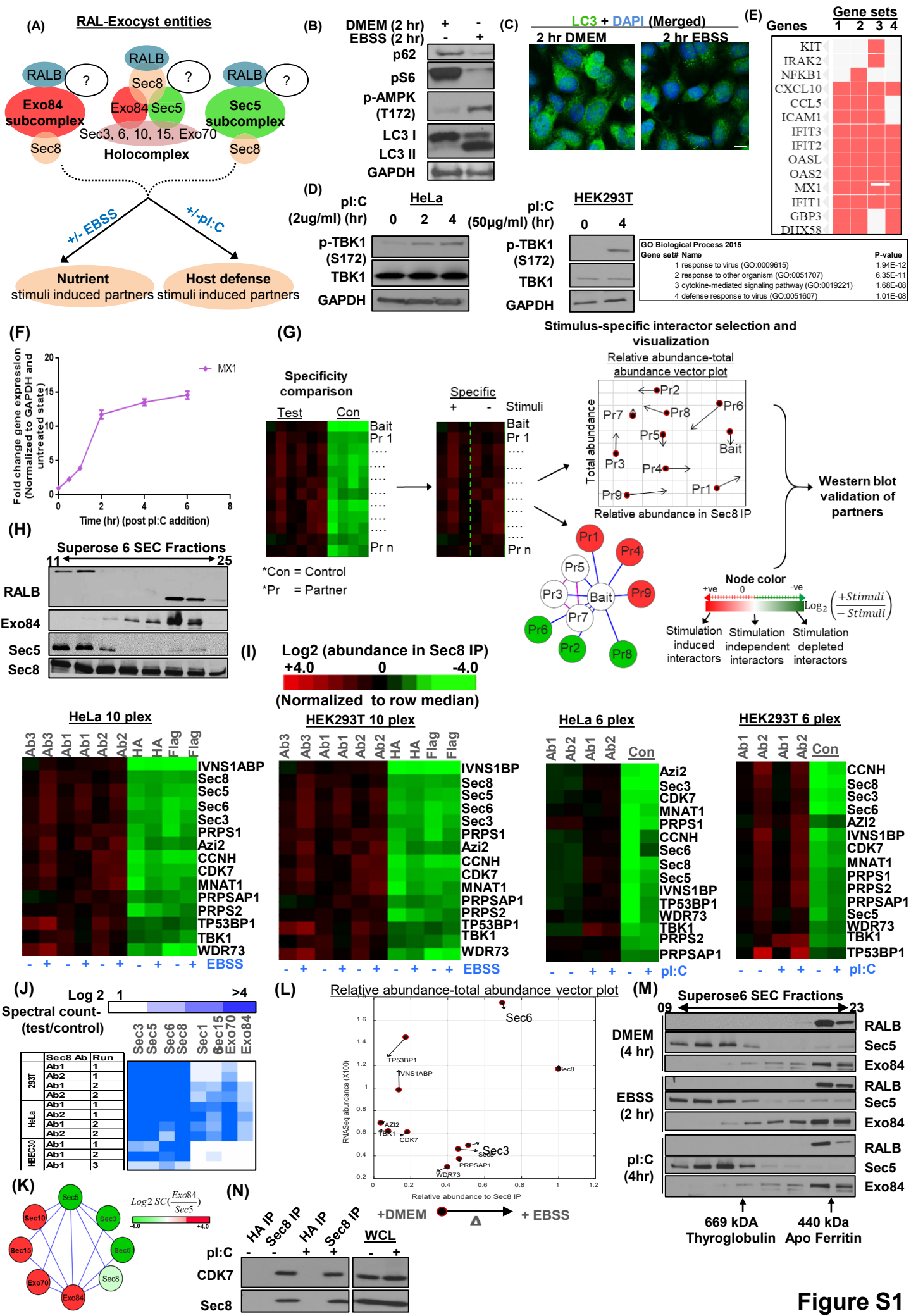
(A)
RAL-Exocyst entities
RALB
Exo84 subcomplex
Sec5 subcomplex
Sec3, 6, 10, 15, Exo70
Holocomplex
Sec8
Exo84
Sec5
+/- EBSS
+/-pI:C
Nutrient stimuli induced partners
Host defense stimuli induced partners
(B)
DMEM (2 hr)
EBSS (2 hr)
p62
pS6
p-AMPK (T172)
LC3 I
LC3 II
GAPDH
(C)
LC3 + DAPI (Merged)
2 hr DMEM
2 hr EBSS
(D)
pI:C (2ug/ml) (hr)
HeLa
p-TBK1 (S172)
TBK1
GAPDH
pI:C (50µg/ml) (hr)
HEK293T
(E)
Genes
Gene sets
KIT
IRAK2
NFKB1
CXCL10
CCL5
ICAM1
IFIT3
IFIT2
OASL
OAS2
MX1
IFIT1
GBP3
DHX58
GO Biological Process 2015
Gene set# Name P-value
1 response to virus (GO:0009615) 1.94E-12
2 response to other organism (GO:0051707) 6.35E-11
3 cytokine-mediated signaling pathway (GO:0019221) 1.68E-08
4 defense response to virus (GO:0051607) 1.01E-08
(F)
MX1
Fold change gene expression (Normalized to GAPDH and untreated state)
Time (hr) (post pI:C addition)
(G)
Stimulus-specific interactor selection and visualization
Specificity comparison
Test
Con
Specific
Stimuli
Bait
Pr 1
Pr n
*Con = Control
*Pr = Partner
Relative abundance-total abundance vector plot
Total abundance
Relative abundance in Sec8 IP
Western blot validation of partners
Node color
Log2 (+Stimuli / −Stimuli)
Stimulation induced interactors
Stimulation independent interactors
Stimulation depleted interactors
(H)
Superose 6 SEC Fractions
RALB
Exo84
Sec5
Sec8
(I)
Log2 (abundance in Sec8 IP)
(Normalized to row median)
HeLa 10 plex
HEK293T 10 plex
HeLa 6 plex
HEK293T 6 plex
EBSS
pI:C
(J)
Log 2 Spectral count-(test/control)
Sec8 Ab
Run
293T
HeLa
HBEC30
(K)
Log2 SC(Exo84/Sec5)
(L)
Relative abundance-total abundance vector plot
RNASeq abundance (X100)
Relative abundance to Sec8 IP
(M)
Superose6 SEC Fractions
DMEM (4 hr)
EBSS (2 hr)
pI:C (4hr)
669 kDa Thyroglobulin
440 kDa Apo Ferritin
(N)
HA IP
Sec8 IP
WCL
+DMEM
+ EBSS
CDK7
Sec8

Figure S1

Figure S1. Distinct exocyst subcomplexes and dynamic alteration of their neighborhood, related to Figure 1.

(A) Schematic illustration of the Ral-exocyst complexes and the strategy for AP-MS as a discovery platform to identify novel context specific exocyst interacting proteins.

(B and C) Cellular response to nutrient challenge. HEK293T cells were incubated with growth media without serum or Earle's basic saline solution (EBSS) as indicated. Whole cell lysates were analyzed for the indicated proteins using SDS-PAGE **(B);** endogenous LC3 was visualized in fixed cells using an established anti-LC3 antibody (number of cells >50) **(C)**.

(D, E and F) Cellular response to dsRNA analog polyI:C or Sendai virus. (D) HeLa and HEK293T cells incubated with pI:C for the indicated time periods were collected and analyzed for the indicated proteins using SDS-PAGE. **(E)** Whole transcriptomes from HeLa cells treated with pI:C and SeV were evaluated individually (data summarized as follows - only pI:C gene sets: KEGG NF-kappa B signaling pathway: $p<0.01$; IRF3 pathway: $p<0.01$; only SeV gene set: KEGG NF-kappa B signaling pathway: $p<0.01$) and combined **(E)** for stimulus-specific enrichments of gene ontologies. Significant genes sets are shown together with leading-edge genes. p-values indicate significance of overlap for hypergeometric density distribution. **(F)** MX1, an established IFN-β response gene, was measured by rtPCR for transcript abundance over time after pI:C challenge. Error bars are Mean ± SD.

(G) AP-MS analysis pipeline. Test and control antibody immunoprecipitates from baseline, nutrient challenged and pI:C challenged samples were characterized by LC-MS. Specificity was defined by enrichment in test samples over controls. Stimulus specific fold change for each interacting protein was measured and visualized either as a relative abundance versus total abundance vector plot or as a network (see methods for details). Candidate partner bait interaction was validated using IP western blot.

(H) Exocyst subunit partition profile. Size exclusion column chromatography fractions of high molecular weight complexes in HEK293T cells were analyzed for the partition profile of the indicated proteins using SDS-PAGE. Data are representative of 3 independent replicates.

(I) Intensity profile of the Sec8 core complex members. Heatmaps represent intensity profile (row median normalized) of the core complex components in HEK293T and HeLa cells.

(J) Sec8 affinity purification recovers all known subunits of the exocyst holocomplex. Sec8 was immunoprecipitated using two epitope specific antibodies in three human epithelial cell lines

and analyzed for spectral count abundance of known exocyst subunits using MS/MS. The heatmap indicates log2 fold enrichment of exocyst subunits in test versus control antibody conditions. Row labels describe cell lines, antibody ID and replicate information for the immunoprecipitates.

(K) Selective enrichment of exocyst subunits between Exo84 and Sec5. Epitope tagged Exo84 and Sec5 were immunoprecipitated (n=8) from HEK293T cells and analyzed for coimmunoprecipitation of exocyst subunits using LC-MS. The results were merged and displayed as a network. The color bar indicates Node color indicates enrichment score, with green centered on Sec5 and red centered on Exo84.

(L) Stimulus-dependent effects on the Sec8 interactome. Nutrient challenge-specific relative abundance versus total abundance vector plot of core Sec8 complex members is shown. Filled circles indicate pre-stimulus values and arrowheads indicate post-stimulus values.

(M) Exocyst subcomplex partition profile under nutrient and immune stimuli. High molecular weight complexes from HEK293T cells, treated as indicated, were isolated using Supersoe6 size exclusion column chromatography and the partition profiles for the indicated proteins were analyzed using SDS-PAGE.

(N) CDK7-Sec8 interaction is independent of pI:C challenge. HEK293T cells were incubated with growth media or pI:C and endogenous Sec8 was immunoprecipitated and analyzed for coimmunoprecipitation of CDK7. Data are representative of 3 independent replicates.

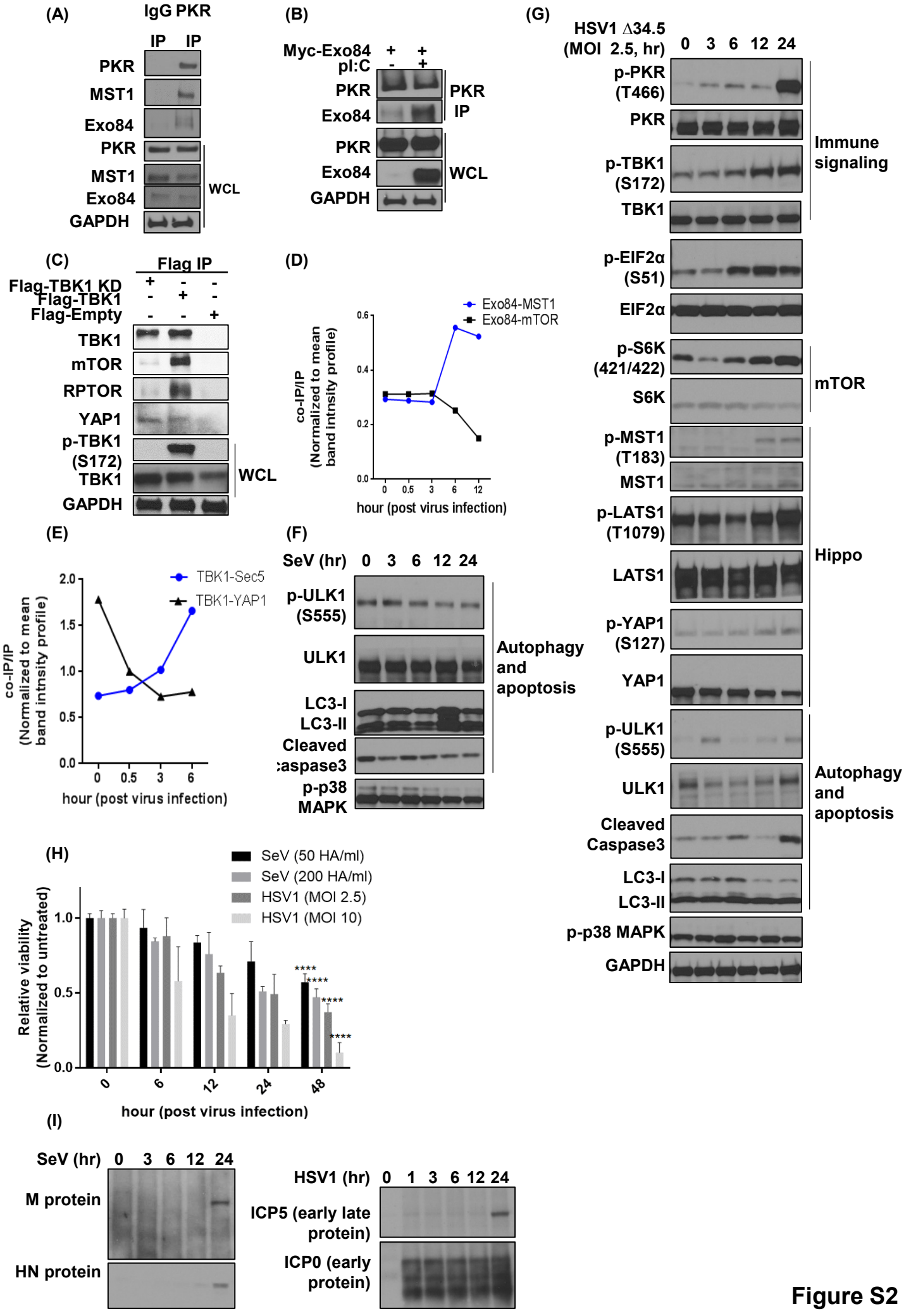
(A)
IgG PKR
IP IP
PKR
MST1
Exo84
PKR
MST1
Exo84
GAPDH
WCL
(B)
Myc-Exo84 + +
pI:C - +
PKR
Exo84
PKR IP
PKR
Exo84
GAPDH
WCL
(C)
Flag IP
Flag-TBK1 KD + - -
Flag-TBK1 - + -
Flag-Empty - - +
TBK1
mTOR
RPTOR
YAP1
p-TBK1 (S172)
TBK1
GAPDH
WCL
(D)
Exo84-MST1
Exo84-mTOR
co-IP/IP (Normalized to mean band intnsity profile)
hour (post virus infection)
(E)
TBK1-Sec5
TBK1-YAP1
co-IP/IP (Normalized to mean band intnsity profile)
hour (post virus infection)
(F)
SeV (hr) 0 3 6 12 24
p-ULK1 (S555)
ULK1
LC3-I
LC3-II
Cleaved caspase3
p-p38 MAPK
Autophagy and apoptosis
(G)
HSV1 Δ34.5 (MOI 2.5, hr) 0 3 6 12 24
p-PKR (T466)
PKR
p-TBK1 (S172)
TBK1
Immune signaling
p-EIF2α (S51)
EIF2α
p-S6K (421/422)
S6K
mTOR
p-MST1 (T183)
MST1
p-LATS1 (T1079)
LATS1
p-YAP1 (S127)
YAP1
Hippo
p-ULK1 (S555)
ULK1
Cleaved Caspase3
LC3-I
LC3-II
Autophagy and apoptosis
p-p38 MAPK
GAPDH
(H)
SeV (50 HA/ml)
SeV (200 HA/ml)
HSV1 (MOI 2.5)
HSV1 (MOI 10)
Relative viability (Normalized to untreated)
hour (post virus infection)
(I)
SeV (hr) 0 3 6 12 24
M protein
HN protein
HSV1 (hr) 0 1 3 6 12 24
ICP5 (early late protein)
ICP0 (early protein)

Figure S2

Figure S2. Characterization of ternary complexes assembled on exocyst subcomplexes and candidate downstream signaling, related to Figure 2.

(A) PKR interacts with MST1 and Exo84. Endogenous PKR immunoprecipitated samples were analyzed by SDS-PAGE for coimmunoprecipitation of indicated proteins. Data are representative of 3 independent replicates.

(B) PKR immunoprecipitation of Exo84 is stimulus sensitive. HEK293T cells ectopically expressing Myc-tagged Exo84 were treated with pI:C for indicated hours and endogenous PKR was immunoprecipitated from confluent cells. The indicated proteins were analyzed for coimmunoprecipitation using SDS-PAGE. Data are representative of 2 independent replicates.

(C) TBK1 interacts with mTOR and YAP1. Flag tagged active TBK1, kinase dead (KD) TBK1 or empty vector were expressed in HEK293T cells and immunoprecipitation was performed using an anti-Flag antibody. Immunoprecipitates were analyzed for coimmunoprecipitation of the indicated proteins. Data are representative of 2 independent replicates.

(D) Kinetics of Exo84-MST1/mTOR interaction. Interaction kinetics was analyzed by quantifying band intensities in **Figure 2C** and **D,** followed by normalized to mean band intensity profile. Data is represented as a line plot.

(E) Kinetics of TBK1-Sec5/YAP1 interaction. Interaction kinetics was analyzed by quantifying band intensities in **Figure 2E** and **F,** followed by normalized to mean band intensity profile. Data is represented as a line plot.

(F) Sendai virus infection induces Hippo signaling, but not autophagy. HEK293T cells infected with Sendai virus for indicated time periods. Cell lysates were analyzed for levels of the indicated proteins using SDS-PAGE. Data are representative of 2 independent replicates.

(G) Kinetic analysis of HSV1 infection on cellular pathways. HEK293T cells infected with HSV1 Δ34.5 (MOI 2.5) for the indicated time periods. Cells were collected to analyze for levels of the indicated proteins using SDS-PAGE. Data are representative of 2 independent replicates.

(H) Toxicity kinetics of SeV and HSV1. HEK293T cells were infected with two different doses of SeV and HSV1 viruses for the indicated time periods and surviving fractions were measured using a standard Cell Titer Glo assay. Data are represented as a histogram with Mean ± SD where n=3. **** denotes statistical significance between the 48 hr time point and 0 hr time point using Student's t test where $p<0.001$.

(I) SeV and HSV1 viral protein expression kinetics. HEK293T cells were infected with SeV (50 HA/ml) and HSV1 (MOI 2.5) for the indicated time periods. Cells were collected to analyze for levels of the indicated proteins using SDS-PAGE. Data are representative of 2 independent replicates.

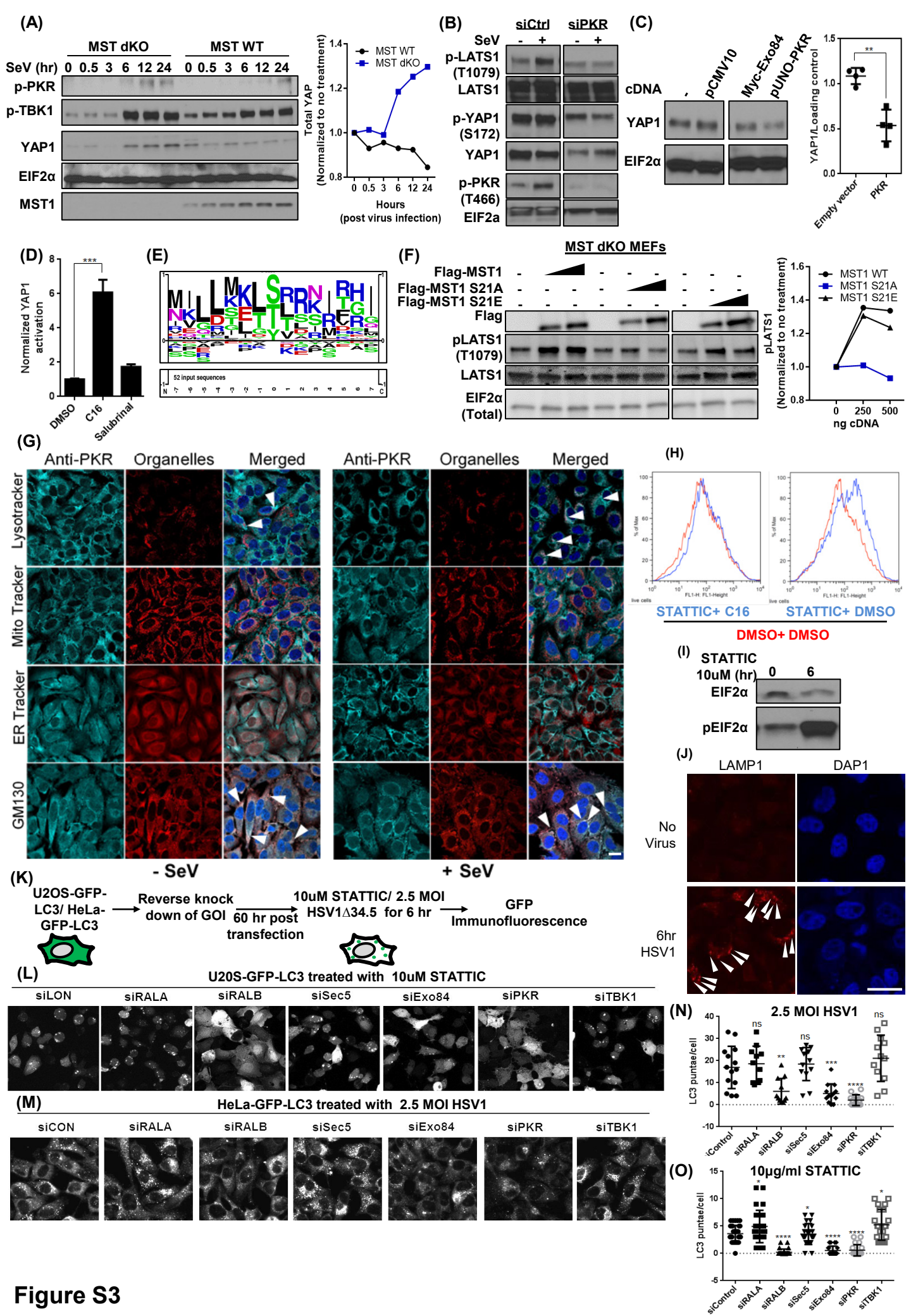
(A)
MST dKO
MST WT
SeV (hr) 0 0.5 3 6 12 24 0 0.5 3 6 12 24
p-PKR
p-TBK1
YAP1
EIF2α
MST1
MST WT
MST dKO
Total YAP
(Normalized to no treatment)
Hours
(post virus infection)
(B)
siCtrl
siPKR
SeV - + - +
p-LATS1 (T1079)
LATS1
p-YAP1 (S172)
YAP1
p-PKR (T466)
EIF2a
(C)
cDNA
pCMV10
Myc-Exo84
pUNO-PKR
YAP1
EIF2α
YAP1/Loading control
Empty vector
PKR
(D)
Normalized YAP1 activation
DMSO
C16
Salubrinal
(E)
52 input sequences
(F)
MST dKO MEFs
Flag-MST1
Flag-MST1 S21A
Flag-MST1 S21E
Flag
pLATS1 (T1079)
LATS1
EIF2α (Total)
MST1 WT
MST1 S21A
MST1 S21E
pLATS1 (Normalized to no treatment)
ng cDNA
(G)
Anti-PKR
Organelles
Merged
Lysotracker
Mito Tracker
ER Tracker
GM130
- SeV
+ SeV
(H)
STATTIC+ C16
STATTIC+ DMSO
DMSO+ DMSO
(I)
STATTIC 10uM (hr) 0 6
EIF2α
pEIF2α
(J)
LAMP1
DAP1
No Virus
6hr HSV1
(K)
U2OS-GFP-LC3/ HeLa-GFP-LC3
Reverse knock down of GOI
60 hr post transfection
10uM STATTIC/ 2.5 MOI HSV1Δ34.5 for 6 hr
GFP Immunofluorescence
(L)
U20S-GFP-LC3 treated with 10uM STATTIC
siLON
siRALA
siRALB
siSec5
siExo84
siPKR
siTBK1
(M)
HeLa-GFP-LC3 treated with 2.5 MOI HSV1
siCON
siRALA
siRALB
siSec5
siExo84
siPKR
siTBK1
(N)
2.5 MOI HSV1
LC3 puntae/cell
siControl
siRALA
siRALB
siSec5
siExo84
siPKR
siTBK1
(O)
10µg/ml STATTIC
LC3 puntae/cell

Figure S3

Figure S3. Functional consequence of PKR/MST1 protein complex assembly on Exo84 subcomplex, related to Figure 3.

(A) MST deficiency cause defect in virus infection mediated YAP1 suppression. MST1/2 deficient (MST dKO) and proficient MEFs were treated with SeV for indicated hours. Harvested cells were probed for level of indicated proteins using SDS-PAGE. Total YAP1 band intensity was quantified and represented as a line plot.

(B) PKR depletion abrogates LATS1 activity. HEK293T cells were reverse transfected with the indicated short interfering RNAs and were incubated with Sendai virus for 10 hr. Cell lysates were analyzed for indicated proteins using SDS-PAGE. Western blot images run on the same membrane were analyzed for comparison. Data are representative of 2 independent replicates.

(C) PKR is sufficient to reduce YAP1 stability. Non-confluent HEK293T cells transiently expressing the indicated constructs were grown to confluence and then incubated with EBSS for 1 hour followed by incubation with DMEM for 30 minutes to induce YAP1 activity. Lysates were collected from each sample and analyzed for the indicated proteins using SDS-PAGE. Data are represented as a histogram with Mean ± SD. Statistical comparison between treatment cohorts was measured using a Student's t test where p value < 0.01. Western blot images run on the same membrane were analyzed for comparison. Data are representative of 4 independent replicates.

(D) Hippo pathway downregulation mediated by PKR inhibition is EIF2α independent. HEK293T cells transiently dual transfected with 8XGTIIC-luc luciferase regulating firefly luciferase and CMV promoter regulated renilla luciferase reporter were treated 6 hours with IC50 dose of C16 and Salubrinal (EIF2αi) or vehicle control (DMSO). The reporter activity was measured by specific/control luminescence signal ratio. Data were normalized to vehicle treatment. Statistical comparison between treatment cohorts were measured using a Student's t test where p value < 0.001, where n=3.

(E) PKR recognition motif. The sequence recognition motif for PKR is represented as a logo based on 52 input sequences from PhosphoSitePlus database.

(F) MST1 S21A mutants are incapable of engaging downstream Hippo signaling kinase LATS1. MST dKO MEFs were transfected with titrating amounts of MST1 wildtype or MST1 S21A or MST21E mutant cDNA expressing plasmids and grown to 90% confluency. Cell lysates were collected and probed for indicated proteins using SDS-PAGE. Western blot images run on the

same membrane were juxtaposed for comparison purpose. Band intensities collected from two independent replicates were quantified and represented as Mean ± SD in a trendline plot.

(G) Colocalization of PKR with cellular organelles. HeLa cells grown on coverslips were fixed and stained with fluorophore conjugated organelle markers and PKR antibody. For Golgi localization GM130 antibody was used. Alexa Fluor 488 against anti-PKR raised in rabbit Alexa fluor 694 against anti-GM130 raised in mouse was used. DAPI (488nm) indicates the nucleus. Colocalization was analyzed by confocal microscopy. Images are pseudocolored and superimposed for colocalization analysis. White arrowheads highlight few areas of colocalizations in the field of view. Number of cells viewed >100. Scale bar indicates 20μm.

(H and I) STATTIC induces PKR mediated autophagy. (H) U2OS cells stably transfected with GFP tagged LC3 construct were grown to confluence and treated 10 hour with 2 μM of the indicated compounds. Cells were collected and Single-cell fluorescence intensity was measure for GFP positive cells. Sample annotation font color is paired with single-cell fluorescence intensity profile. **(I)** In a parallel experiment confluent HeLa cells were incubated with 10μM of the STATTIC and were analyzed for the proteins indicated using SDS-PAGE.

(J) HSV1 infection causes lysosome nucleation. HeLa cells were infected with or without HSV1 ∆34.5 for 6 hour. Fixed cells were analyzed for immunofluorescence for LAMP1- a lysosomal marker. White arrowheads highlight few LAMP1 puncta in the field of view. Number of cells viewed >50. Scale bar indicates 20μm.

(K, L, M, N and O) Exo84 and RALB are required for PKR induced xenophagy. (K) Schematic representation for immunofluorescence-based analysis for identifying genetic components necessary for virus and STATTIC mediated autophagy. **(L)** U2OS-LC3-GFP cells were transiently transfected with indicated siRNAs and grown to confluence before treatment with 10μM of the STATTIC. Cell were fixed and analyzed for accumulation of GFP-LC3 puncta/cells. **(M)** HeLa cells were reverse transfected with indicated short interfering RNAs and were incubated with growth media with or without HSV∆34.5 mutant (MOI 2.5) for 6 hours. Cell were fixed and analyzed for accumulation of LC3 puncta/cells using endogenous LC3 antibody. Scale bar indicates 20μm. **(N and O)** Puncta from 15 representative cells from 5 different images for each condition were used to generate statistical significance. Statistical analysis for the puncta/cells for **L** and **M** were quantified, represented as Mean ± SEM and compared between the cohorts using unpaired student's t test (****=p<0.001, ***=p<0.05, **=p<0.01 and *p<0.05).

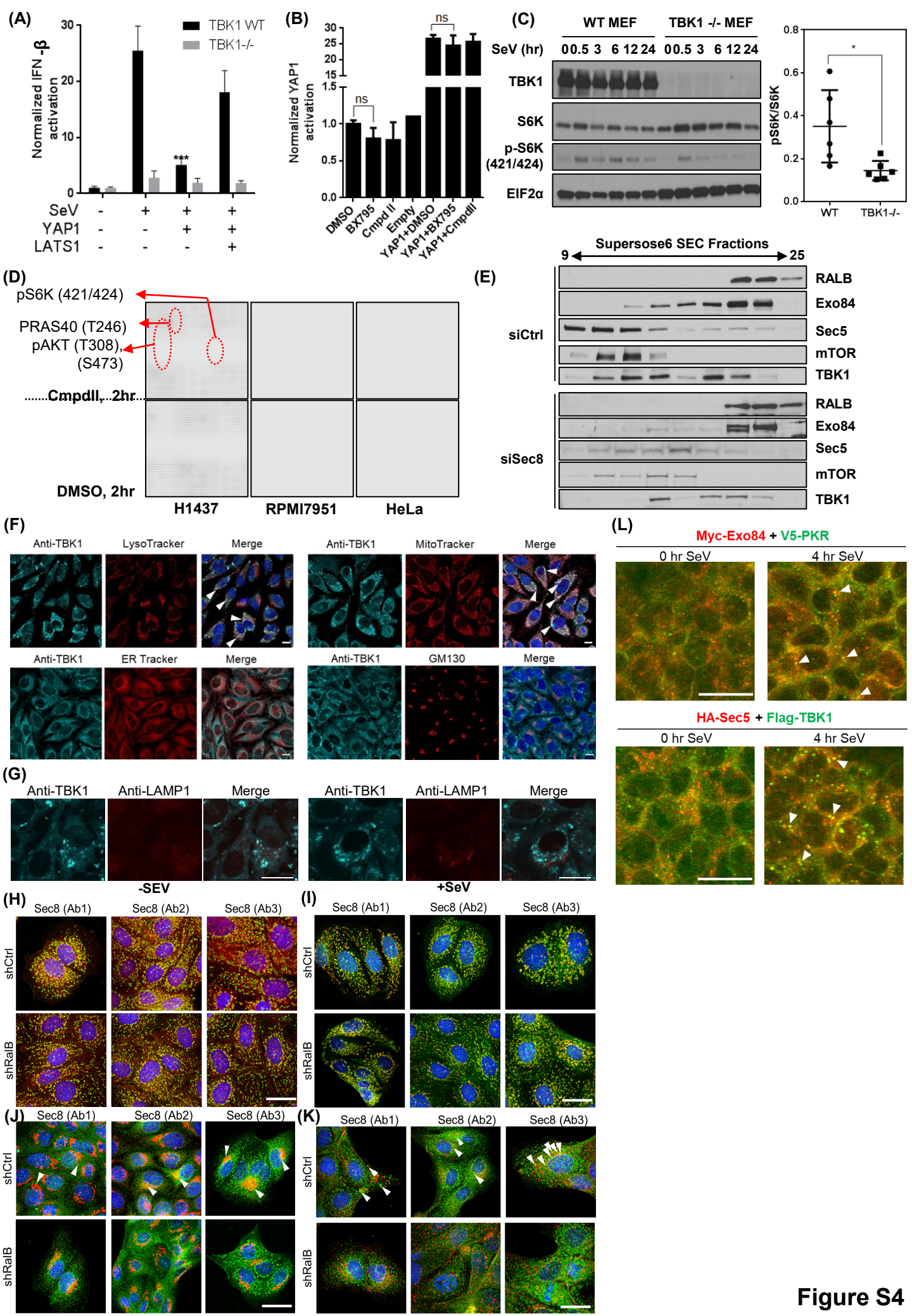
(A)
Normalized IFN-β activation
TBK1 WT
TBK1-/-
***
SeV - + + +
YAP1 - - + +
LATS1 - - - +
(B)
Normalized YAP1 activation
ns
ns
DMSO
BX795
Cmpd II
Empty
YAP1+DMSO
YAP1+BX795
YAP1+CmpdII
(C)
WT MEF
TBK1 -/- MEF
SeV (hr)
0 0.5 3 6 12 24 0 0.5 3 6 12 24
TBK1
S6K
p-S6K (421/424)
EIF2α
pS6K/S6K
*
WT
TBK1-/-
(D)
pS6K (421/424)
PRAS40 (T246)
pAKT (T308), (S473)
Cmpdll, 2hr
DMSO, 2hr
H1437
RPMI7951
HeLa
(E)
Supersose6 SEC Fractions
9
25
siCtrl
siSec8
RALB
Exo84
Sec5
mTOR
TBK1
(F)
Anti-TBK1
LysoTracker
Merge
MitoTracker
ER Tracker
GM130
(G)
Anti-LAMP1
-SEV
+SeV
(H)
(I)
Sec8 (Ab1)
Sec8 (Ab2)
Sec8 (Ab3)
shCtrl
shRalB
(J)
(K)
(L)
Myc-Exo84 + V5-PKR
0 hr SeV
4 hr SeV
HA-Sec5 + Flag-TBK1

Figure S4

Figure S4. Functional consequence of Sec5/TBK1 protein complex assembly on Sec5 subcomplex, related to Figure 4.

(A) YAP1 inhibits the IFN-β response. HEK293T cells were transiently transfected with IFN-β promoter regulated firefly luciferase and CMV promoter regulated renilla luciferase reporters. Cells were treated with or without 6 hours of exposure to 50 HA/mL of SeV. IFN-β activation was measured using a standard dual luciferase assay. Data are represented as a histogram with Mean ± SD where n=3. Statistical comparison between treatment cohorts were measured using a Student's t test where p value < 0.005.

(B) TBK1 mediated regulation of YAP1 is kinase independent. HEK293T cells were transiently transfected with 8XGTIIC-luc firefly luciferase, renilla luciferase reporters along with indicated cDNAs and/or treated 6 hours with an ED50 dose of TBK1 inhibitors BX795 or Cmpd II or vehicle control (DMSO). YAP1 activation was measured using a standard dual luciferase assay. Data are represented as a histogram with Mean ± SD where n=3. Statistical comparison between treatment cohorts was measured using a Student's t test.

(C) TBK1 null (-/-) MEFs fail to sustain mTOR activation under immune challenge. Near confluent cultures of TBK1 wildtype and TBK1 null MEFs were incubated with 200 µg/ml Sendai virus for the indicated hours. Lysates were collected and analyzed for the indicated proteins using SDS-PAGE. From two independent replicates, the "12 hour" as well as "24 hour" treatment band intensities were grouped and compared with that of "0 hr treatment" treatment cohort. Statistical comparison between treatment cohorts (Mean ± SEM) was measured using a Student's t test where p value < 0.05.

(D) Cmpd II (TBK1 inhibitor) ablates PRAS40, AKT and S6K phosphorylation. Representation of DMSO and CmpdII treated phosphor-ELISA array images two replicates in 2 CmpdII resistant cell lines (H1437 and RPMI7951) in **Figure 4H** and one sensitive cell line (HeLa). The most differentially regulated phosphorylation events are marked as red ellipses.

(E) Sec8 knockdown disrupts the Sec5/mTOR/TBK1 complex. HEK293T cells reverse transfected with indicated siRNAs were grown to confluence and high molecular weight complexes were isolated and were analyzed for partition profile of the indicated proteins using supersoe6 size exclusion chromatography. Data are representative of two replicates.

(F) Colocalization of TBK1 with cellular organelles. HeLa cells grown on coverslips were fixed and stained with organelle markers and TBK1 antibody. For Golgi localization GM130 antibody

was used. Alexa Fluor 488 against anti-PKR raised in rabbit Alexa fluor 694 against anti-GM130 raised in mouse was used. DAPI (488nm) indicates the nucleus. Colocalization was analyzed by confocal microscopy. Images are pseudocolored and superimposed for colocalization analysis. White arrowheads highlight few areas of colocalizations in the field of view. Number of cells viewed >100. Scale bar indicates 20μm.

(G) TBK1 colocalizes proximal to lyso-endosomal marker LAMP1. HeLa cells grown on coverslips were fixed and stained with anti-LAMP1 and anti-TBK1 antibody. Alexa Fluor 488 against anti-TBK1 raised in rabbit Alexa fluor 694 against anti-LAMP1 raised in mouse was used. Colocalization was analyzed by confocal microscopy. White arrowheads highlight few areas of colocalizations in the field of view. Number of cells viewed >25. Scale bar indicates 20μm.

(H, I, J and K) Colocalization of Sec8 with cellular organelles. Cells were stained with three monoclonal antibodies against Sec8 (green) and organelle markers **(H)** ER marker ERP29 (red), **(I)**, mitochondria marker AIF (red), **(J)** Golgi marker GM130 (Red) and **(K)** Lysosome marker LAMP1 (Red) in control or RALB abrogated MDCK cells. DAPI (488nm) indicates the nucleus. White arrowheads highlight few areas of colocalizations in the field of view. Number of cells viewed >25. Scale bar indicates 20μm.

(L) Exo84 and Sec5 colocalizes with PKR and TBK1, respectively. Myc-Exo84 and V5-PKR or HA-Sec5 and Flag-TBK1 was coexpressed in HEK293T cells and were stained for tag specific antibodies for colocalization in the presence or absence of SeV stimuli using confocal microscopy. White arrowheads highlight few areas of colocalizations in the field of view. Number of cells viewed >50. Scale bar indicates 20μm.

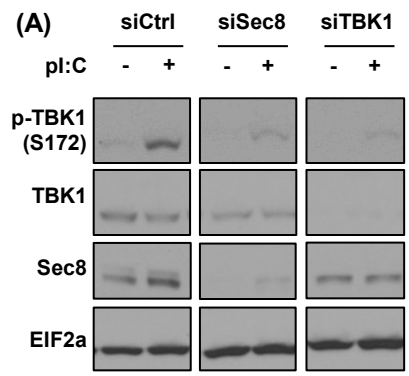
(A)
siCtrl
siSec8
siTBK1
pI:C
- + - + - +
p-TBK1 (S172)
TBK1
Sec8
EIF2a

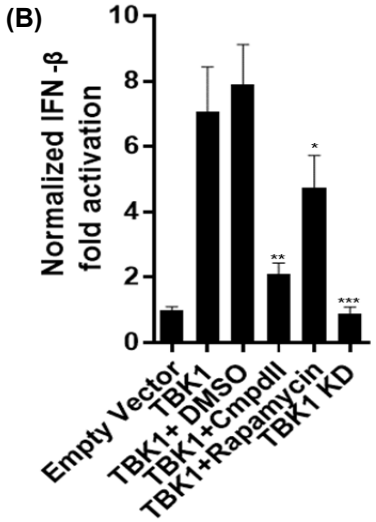
(B)
Normalized IFN-β fold activation
0
2
4
6
8
10
**
*
***
Empty Vector
TBK1
TBK1+ DMSO
TBK1+CmpdII
TBK1+Rapamycin
TBK1 KD

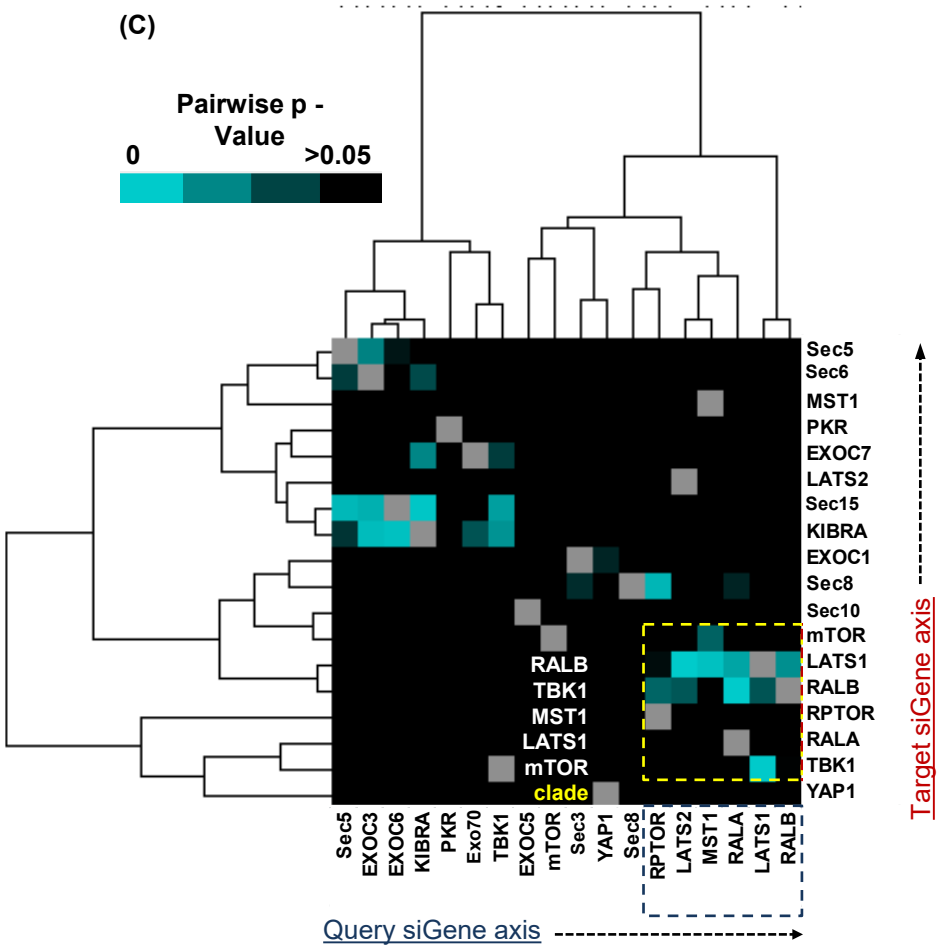
(C)
Pairwise p - Value
0
>0.05
Sec5
Sec6
MST1
PKR
EXOC7
LATS2
Sec15
KIBRA
EXOC1
Sec8
Sec10
mTOR
LATS1
RALB
RPTOR
RALA
TBK1
YAP1
RALB
TBK1
MST1
LATS1
mTOR
clade
Sec5
EXOC3
EXOC6
KIBRA
PKR
Exo70
TBK1
EXOC5
mTOR
Sec3
YAP1
Sec8
RPTOR
LATS2
MST1
RALA
LATS1
RALB
Query siGene axis
Target siGene axis

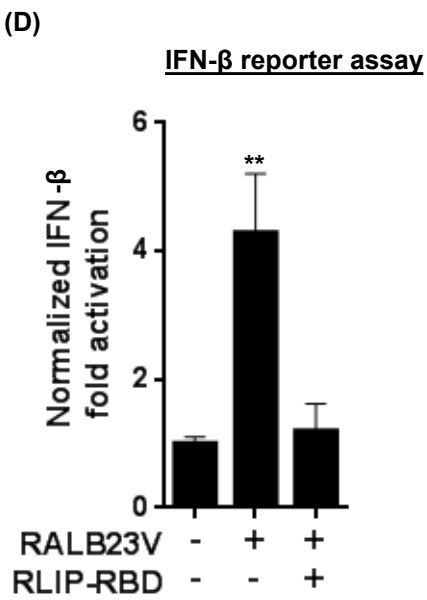
(D)
IFN-β reporter assay
Normalized IFN-β fold activation
0
2
4
6
**
RALB23V - + +
RLIP-RBD - - +

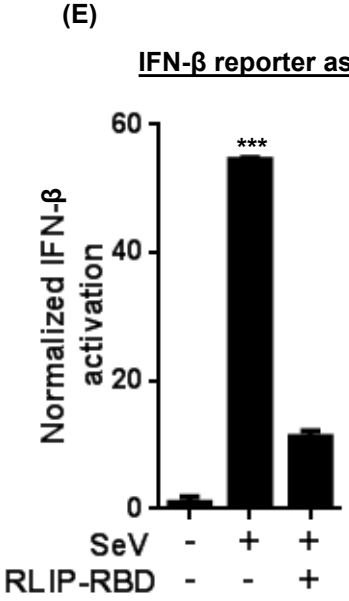
(E)
IFN-β reporter assay
Normalized IFN-β activation
0
20
40
60
***
SeV - + +
RLIP-RBD - - +

Figure S5

Figure S5. RAL-Exocyst signaling axis and their role for hippo and mTOR signaling activation, related to Figure 5.

(A) Sec8 supports immune challenge dependent TBK1 activation. HEK293T cells were reverse transfected with the indicated short interfering RNAs and were incubated with pI:C (2μg/mL) for indicated time periods. Cell lysates were analyzed for indicated proteins using SDS-PAGE. Data are representative of 2 independent replicates.

(B) mTOR activation is necessary for maximal IFN-β promoter activation. HEK293T cells ectopically expressing IFN-β reporter expressing firefly luciferase with a renilla luciferase control and plasmids expressing the indicated cDNA or empty vector were grown for 24 hours and normalized IFN-β promoter induction was measured using a standard dual luciferase assay. KD stands for kinase dead. Data are represented as a histogram representing mean ± SD, where n=3. Statistical significance between 'TBK1+DMSO' cohort and the other cohorts were measured by using unpaired Student's t-test (***= p<0.001; **=p<0.01, *=p<0.05)

(C) Functional relationship between RAL-exocyst and Hippo signaling using FUSION datasets. Functional association between exocyst subunits, core Hippo pathway proteins and mTOR related hits were calculated using the FUSION1.5 dataset by measuring the similarity between gene knockdown effects expressed as a 6 gene reporter feature (Potts, Kim *et. al.* 2013). For a query gene knock down pair-wise p value for each of the rest of the 'target genes' in the list were exported from the database and an asymmetric square matrix (where effect of query knockdown to target gene ≠ effect of target gene knockdown to query gene) was generated. p-value was capped as insignificant for any value above at 0.05. The generated matrix was 2 way-clustered to identify genes behaving most similarly within the curated list of proteins.

(D) RALB is sufficient to induce IFN-β promoter activation. U2OS cells overexpressing IFN-β promoter regulating firefly luciferase, CMV promoter regulated renilla luciferase along with the indicated cDNAs were subjected to a standard reporter dual luciferase assay. Normalized IFN-β activation fold changes are represented as histograms representing Mean ± SD. Significance for the three independent replicates of the comparison cohorts was measured using an unpaired Students t-test. * (asterisks) indicates p<0,05 and ** indicates p<0.01, where n=3.

(E) RALB is required to induce IFN-β promoter activity. HEK293T cells overexpressing IFN-β overexpressing 8XGTIIC-luc promoter regulating firefly luciferase, CMV promoter regulated renilla luciferase along with the indicated cDNAs were incubated with 200 HA/ml SeV for 12 hours followed by a standard reporter dual luciferase assay. Normalized IFN-β activation fold changes

are represented as histograms representing Mean ± SD. Significance for the three independent replicates of the comparison cohorts was measured using an unpaired Students t-test. (*=p<0,05 and ***=p<0.005, n=3).

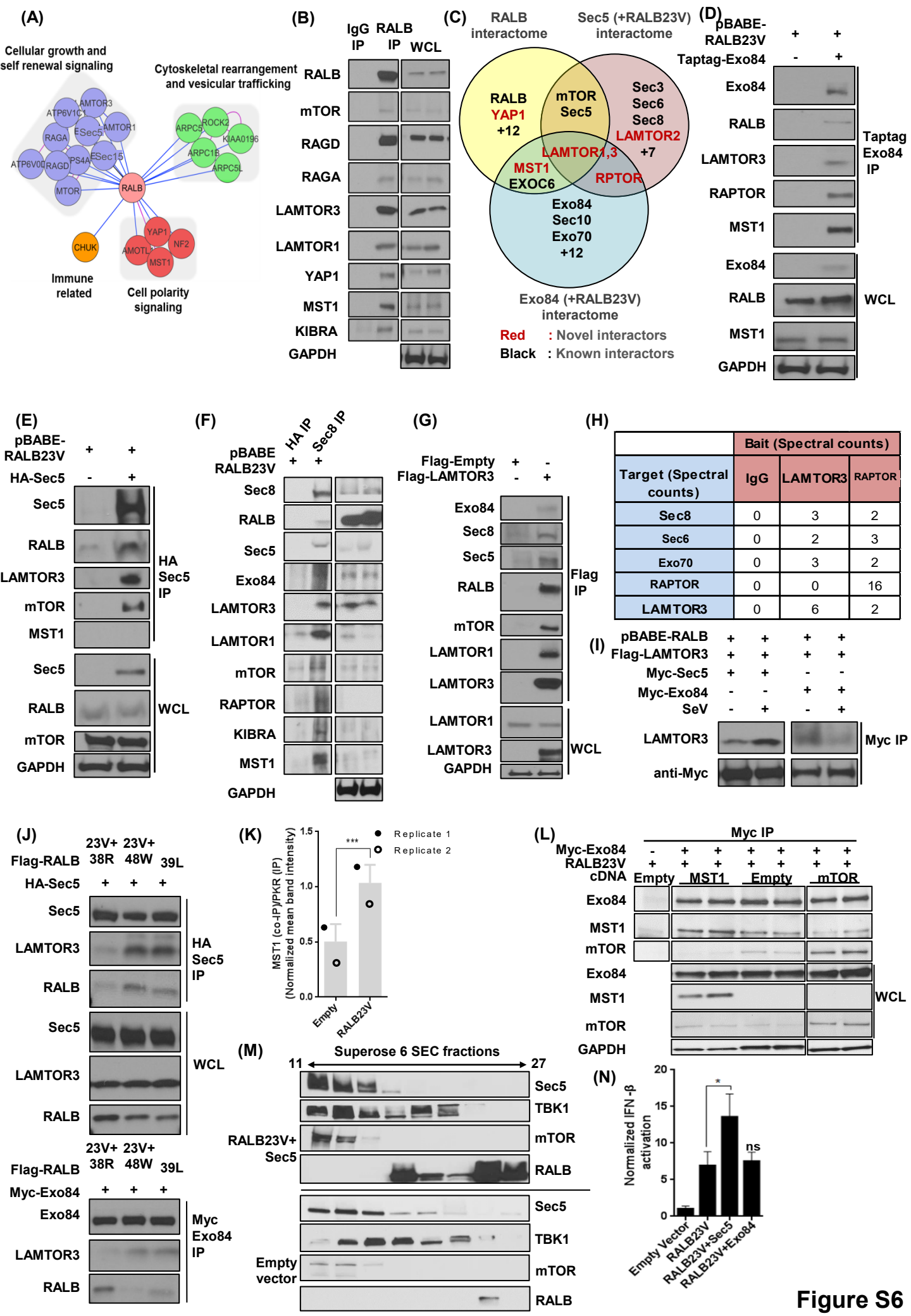
(A)
Cellular growth and self renewal signaling
Cytoskeletal rearrangement and vesicular trafficking
Immune related
Cell polarity signaling
(B)
IgG IP
RALB IP
WCL
RALB
mTOR
RAGD
RAGA
LAMTOR3
LAMTOR1
YAP1
MST1
KIBRA
GAPDH
(C)
RALB interactome
Sec5 (+RALB23V) interactome
Exo84 (+RALB23V) interactome
RALB YAP1 +12
mTOR Sec5
Sec3 Sec6 Sec8 LAMTOR2 +7
LAMTOR1,3
MST1 EXOC6
RPTOR
Exo84 Sec10 Exo70 +12
Red : Novel interactors
Black : Known interactors
(D)
pBABE-RALB23V
Taptag-Exo84
Exo84
RALB
LAMTOR3
RAPTOR
MST1
Taptag Exo84 IP
WCL
GAPDH
(E)
pBABE-RALB23V
HA-Sec5
Sec5
RALB
LAMTOR3
mTOR
MST1
HA Sec5 IP
WCL
GAPDH
(F)
HA IP
Sec8 IP
pBABE RALB23V
Sec8
RALB
Sec5
Exo84
LAMTOR3
LAMTOR1
mTOR
RAPTOR
KIBRA
MST1
GAPDH
(G)
Flag-Empty
Flag-LAMTOR3
Exo84
Sec8
Sec5
RALB
mTOR
LAMTOR1
LAMTOR3
Flag IP
WCL
GAPDH
(H)
Bait (Spectral counts)
Target (Spectral counts)
IgG
LAMTOR3
RAPTOR
Sec8 0 3 2
Sec6 0 2 3
Exo70 0 3 2
RAPTOR 0 0 16
LAMTOR3 0 6 2
(I)
pBABE-RALB
Flag-LAMTOR3
Myc-Sec5
Myc-Exo84
SeV
LAMTOR3
anti-Myc
Myc IP
(J)
Flag-RALB
23V+ 38R
23V+ 48W
39L
HA-Sec5
Sec5
LAMTOR3
RALB
HA Sec5 IP
WCL
Myc-Exo84
Exo84
Myc Exo84 IP
(K)
Replicate 1
Replicate 2
***
MST1 (co-IP)/PKR (IP)
(Normalized mean band intensity)
Empty
RALB23V
(L)
Myc IP
Myc-Exo84
RALB23V
cDNA
Empty
MST1
Empty
mTOR
Exo84
MST1
mTOR
WCL
GAPDH
(M)
Superose 6 SEC fractions
11
27
RALB23V+ Sec5
Empty vector
Sec5
TBK1
mTOR
RALB
(N)
Normalized IFN-β activation
*
ns
Empty Vector
RALB23V
RALB23V+Sec5
RALB23V+Exo84

Figure S6

Figure S6. RALB driven dynamic assembly of Sec5 and Exo84 ternary complexes occur in expense of dissociation of competitive binding effectors, related to Figure 6.

(A and B) RALB core complex identifies MST1 and LAMTORs as novel interactors. (A) Using antibodies specific for RALB, a de-novo RALB interactome was generated using the AP-MS pipeline. The blue edges emanating from RAL represent experimental interactions; pink edges between other nodes represent interactions reported in the BIOGRID database. The nodes were manually classified into different functional groups as indicated using the grey box. **(B)** Western blot validation of the hits from (**A)**.

(C) Active RALB driven exocyst interactome. (Left) Transiently overexpressed Taptag-Exo84 and HA-Sec5 were immunoprecipitated from HEK293T cells stably overexpressing RALB23V. The immunoprecipitates were analyzed for coimmunoprecipitation of proteins using LC-MS. The RALB driven Exo84 and Sec5 interactome was superimposed on the de-novo RAL interactome to generate comparisons represented as an euler plot.

(D, E and F) Western blot validation of active RALB driven Exo84 and Sec5 interactome. Endogenous Sec8, Taptag-Exo84, HA-Sec5 was immunoprecipitated from HEK293T cells in the presence of stable expression of **(D)** RALB23V and Exo84 or **(E)** RALB23V and Sec5 or **(F)** RALB23V, respectively. **(D and E)** Exo84 and Sec5 was immunoprecipitated with antibodies directed to the specified tags. **(F)** Endogenous Sec8 was immunoprecipitated using as established anti-Sec8 antibody. Immunoprecipitates were analyzed for coimmunoprecipitation of the indicated proteins. Data are representative of 2 independent replicates.

(G) LAMTOR3 and mTOR interact with RALB and exocyst holocomplex subunits. HEK293T transiently overexpressing Flag-LAMTOR3 was used to immunoprecipitate LAMTOR3 and the indicated proteins were analyzed for coimmunoprecipitation. Data are representative of 2 independent replicates.

(H) LAMTOR complex components are a common interactor for exocyst and RAPTOR. The table illustrates MS/MS spectral count values of exocyst subunits, LAMTOR3 and RAPTOR identified in LAMTOR3 and RAPTOR interactome. Data are representative of 2 independent replicates.

(I) LAMTOR3 exocyst interaction is stimulus specific. HEK293T cells transiently expressing the indicated cDNA were grown to confluence and treated with SeV for the indicated hours. Exo84 or Sec5 was immunoprecipitated using anti-Myc antibody and analyzed for by

coimmunoprecipitation for the indicated proteins by SDS-PAGE. Data are representative of 2 independent replicates.

(J) RALB drives LAMTOR3 interaction with the exocyst holocomplex and Sec5 subcomplex. Point mutations in RALB23V that that have differential association of RALB with either Exo84 or Sec5 were overexpressed stably in fusion tagged Sec5 expressing HEK293T cells. Sec5 was immunoprecipitated and the indicated proteins were analyzed using SDS-PAGE. Data are representative of 2 independent replicates.

(K) RALB is sufficient to increase the PKR/MST1 interaction. Quantification of two replicates of representative data demonstrated in **Figure 6G.** Normalized mean band intensity for MST1 co-immunoprecipitation with PKR immunoprecipitation was represented as a bar graph. Error bar indicates SD. Statistical significance was measured using a Mann Whitney U test ($p<0.01$).

(L) MST1 and mTOR can competitively dissociate each other from Exo84. Myc-Exo84 and RALB23V expressing HEK293T cells were transfected with either MST1 or empty vector or mTOR overexpression cDNA constructs and grown to confluence and Exo84 was immunoprecipitated using an anti-Myc antibody and analyzed for coimmunoprecipitation of the indicated proteins using SDS-PAGE.

(M) Active RALB and Sec5 co-expression results in distinct high molecular weight complex partition profile for TBK1 and mTOR. HEK293T cells transiently expressing the indicated cDNAs were grown to confluence and cells were collected in gel filtration buffer. Filtered lysates were injected onto a supersoe6 column at 0.2ml/min rate and forty 0.5ml fractions were collected and fractions 13^{th} to 29^{th} were analyzed by SDS-PAGE for the indicated proteins. Data are representative of 2 replicates.

(N) RALB23V and Sec5 co-expression activates IFN-β activity. HEK293T cells ectopically expressing 8XGTIIC-luc luciferase reporter expressing firefly luciferase with a renilla luciferase control and plasmids expressing the indicated cDNA or empty vector were grown for 24 hours and normalized Hippo induction was measured using a standard dual luciferase assay. Data are shown as a histogram representing Mean ± SD. Statistical comparison between the cohorts using three independent replicates was measured using a Student's unpaired t-test where p value < 0.05.

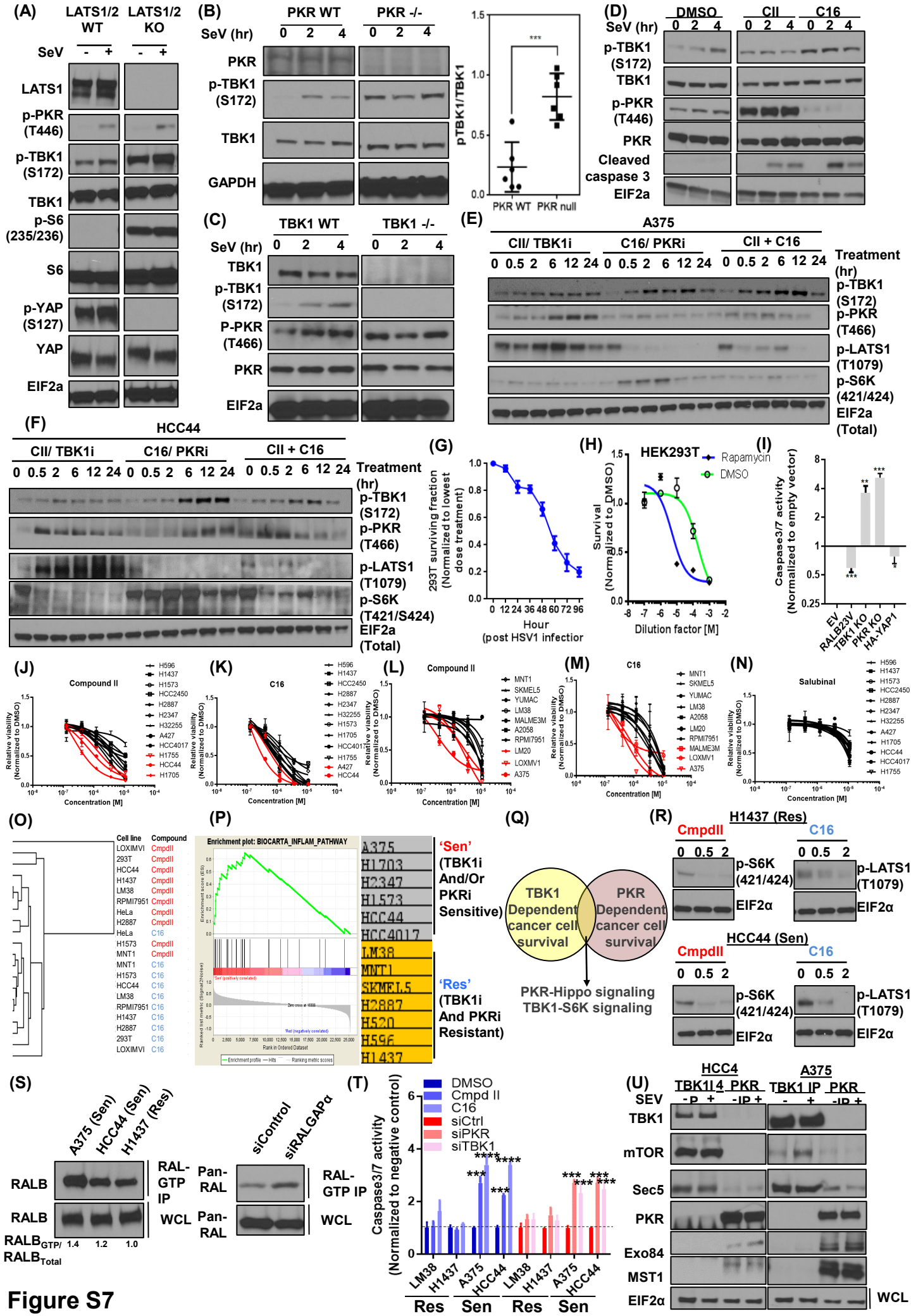
(A)
LATS1/2 WT
LATS1/2 KO
SeV
LATS1
p-PKR (T446)
p-TBK1 (S172)
TBK1
p-S6 (235/236)
S6
p-YAP (S127)
YAP
EIF2a
(B)
PKR WT
PKR -/-
SeV (hr)
PKR
p-TBK1 (S172)
TBK1
GAPDH
pTBK1/TBK1
PKR WT
PKR null
(C)
TBK1 WT
TBK1 -/-
P-PKR (T466)
(D)
DMSO
CII
C16
Cleaved caspase 3
(E)
A375
CII/ TBK1i
C16/ PKRi
CII + C16
Treatment (hr)
p-LATS1 (T1079)
p-S6K (421/424)
(F)
HCC44
(G)
293T surviving fraction (Normalized to lowest dose treatment)
Hour (post HSV1 infection
(H)
HEK293T
Rapamycin
DMSO
Survival (Normalized to DMSO)
Dilution factor [M]
(I)
Caspase3/7 activity (Normalized to empty vector)
EV
RALB23V
TBK1 KO
PKR KO
HA-YAP1
(J)
Compound II
(K)
C16
(L)
(M)
(N)
Salubinal
Relative viability (Normalized to DMSO)
Concentration [M]
(O)
Cell line
Compound
(P)
Enrichment plot: BIOCARTA_INFLAM_PATHWAY
'Sen' (TBK1i And/Or PKRi Sensitive)
'Res' (TBK1i And PKRi Resistant)
(Q)
TBK1 Dependent cancer cell survival
PKR Dependent cancer cell survival
PKR-Hippo signaling
TBK1-S6K signaling
(R)
H1437 (Res)
HCC44 (Sen)
p-S6K (421/424)
p-LATS1 (T1079)
EIF2α
(S)
A375 (Sen)
HCC44 (Sen)
H1437 (Res)
siControl
siRALGAPα
RALB
RAL-GTP IP
WCL
Pan-RAL
RALB_GTP/ RALB_Total
(T)
DMSO
Cmpd II
C16
siCtrl
siPKR
siTBK1
Caspase3/7 activity (Normalized to negative control)
Res
Sen
(U)
HCC4
A375
TBK1 IP
PKR IP
SEV
TBK1
mTOR
Sec5
PKR
Exo84
MST1
EIF2α
WCL

Figure S7

Figure S7. A subset of cancer cells coopts exocyst dependent concomitant activation of hippo and mTOR signaling for cellular survival, related to Figure 7.

(A) High baseline TBK1 and mTOR activity in LATS1/2 knockout cells. LATS1/2 wildtype and knockout 293A cells were grown to confluence and treated as indicated. After treatment, cells were harvested, and lysates were analyzed for the indicated proteins using SDS-PAGE. Western blot images run on the same membrane were used for comparison. Data is representative of 2 replicates

(B and C) High baseline TBK1 activity in PKR null MEFs and vice versa. TBK1 and PKR wildtype and null MEFs were grown to confluence and treated as indicated. After treatment, cells were harvested, and lysates were analyzed for indicated proteins using SDS-PAGE. Significance for comparison between the cohorts was measured using an unpaired Student's t-test (***= $p<0.001$). Western blot images run on the same membrane were used for comparison of p-TBK1/TBK1 ratio between WT and null cohorts. Data is representative of 2 replicates

(D, E and F) TBK1 and PKR inactivation causes upregulation of the other. (D) HeLa and **(E)** A375 (melanoma cell line) and **(F)** HCC44 (lung cancer cell line) cells grown to confluence, pre-treated with vehicle (DMSO), Compound II and C16 for indicated hours, were exposed to Sev for the indicated hours. Lysates were collected from the harvested cells and the protein levels indicated were measured by SDS-PAGE. Western blot images run on the same membrane were used for comparison. Data is representative of 2 replicates

(G) HSV1 toxicity kinetics. HEK293T cells were incubated with 10^6 PFU HSV1 virus stock for indicated hours and their post infection normalized viability was measured where error bars indicate SD and n=3.

(H) mTOR signaling is immune protective. HEK293T cells were pretreated with 0.2μM Rapamycin for 6 hours followed by indicated dilutions of 10^6 PFU HSV1 virus stock. 48 hours post infection relative cell viability was measured using Cell Titer Glo. Dose response curves are plotted from 3 independent replicates and error bars indicate SD.

(I) Role of RALB, YAP, PKR and TBK1 during HSV1 cytotoxicity in isogenic cells. HEK293T cells stably over-expressing RALB23V or HA-YAP and deficient in TBK1 and PKR (through CRISPR mediated knock out) were incubated with HSV1 (MOI 2.5) for 24 hours and analyzed by cellular Caspase 3/7 level using the Caspase Glo reagent. Data are represented as a bar diagram with Mean ± SD where ** indicates $p<0.01$ and ***indicates $p<0.005$.

(J, K, L, M and N) Dose response curves of lung cancer cells and melanoma cells treated with TBK1 inhibitor, Compound II, PKR inhibitor, C16 and EIF2a inhibitor salubrinal. 24-hours post seeding, lung (**J, K and N**) and melanoma (**L and M**) cell lines grown on 96 well plates, were treated for the indicated compounds for an additional 72 hours. Cells were lysed cell viability assessed using the Cell Titer Glo assay and viability was plotted as dose response using 4-parameter non liner curve fitting. Red lines indicate classification of the cell line as sensitive to each of the compounds whereas black indicates resistant cell lines. Each dots in dose response curves represents mean viability where n=3 and error bars represent standard deviation (SD).

(O) Mode of action of PKR inhibitor and TBK1 inhibitor is divergent. 10 different cell lines from lung cancer and melanoma origin were grown to confluence and were treated with vehicle (DMSO), Compound II and C16 for 2 hours. Collected lystaes from the cells were subjected to dot blot protein array that catalogued levels of 35 protein alterations relevant to pathways of cellular growth and immunity (see methods for detail). Intensity of the dot blots was measured. For each protein alteration, the levels in Compound II and C16 exposed cells were normalized to DMSO. Normalized values were used to generate 2-way unsupervised hierarchical clustering. A dendrogram for the clustering of the samples is represented where red indicates Compound II and blue indicates C16 treated cells.

(P) A subset of 'inflammation/immune pathway' dependent cancer cells uses PKR and TBK1 for survival. 17 lung cancer and 10 melanoma cell lines were treated with PKR inhibitor (C16) or TBK1 inhibitor (CmpdII) for 72 hours and cell viability was measured using Cell Titer Glo. The ED50 values for each lineage were separately rank ordered and cell lines with values in the first and third quartile for TBK1 or PKR inhibitor treatments were individually selected. Gene set enrichment analysis (GSEA) was performed comparing cell lines that were TBK1 inhibitor and/or PKR inhibitor sensitive versus resistant. GSEA analysis identified gene set 'BIOCARTA-INFLAM-PATHWAY' as the most enriched gene sets (NES=0.65)

(Q) Representation of a strategy for identifying TBK1 and PKR mediated promotion of tumor cell viability. Schematic Venn diagram outlining hypothesized overlap between the PKR and TBK1 mediated cell viability. TBK1 inhibitor (CmpdII) and PKR inhibitor (C16) IC50 values obtained from 17 lung cancer and 10 melanoma cell lines were measured and used for defining this cohort.

(R) PKR ablation causes LATS1 downregulation whereas TBK1 ablation causes S6K downregulation in cancer cells. The indicated cell lines were treated with indicated compounds

for the hours indicated. Lysates were collected and were analyzed by Western blot for indicated proteins.

(S) 'Immune pathway dependent' cancer cell lines with high PKR and TBK1 activity show high RALB activity. Active RALB present in the indicated cell lines was immunoprecipitated using GST-RBD and analyzed for the indicated proteins in immunoprecipitates and whole cell lysates. As an assay control, active RALB from HEK293T cells reverse transfected with indicated siRNAs were immunoprecipitated using GST-Sec5-RBD and analyzed for indicated proteins in immunoprecipitates and whole cell lysates. Band intensities were measured for quantification of relative RALB-GTP level.

(T) Genetic and pharmacological TBK1 and PKR perturbation causes apoptosis in 'immune pathway dependent' lines. Indicated cells were incubated with the compounds for 36 hours and cleaved caspase 3 level- a marker for apoptosis- was measured by Caspase Glo fluorescent read out. Normalized caspase 3/7 level is illustrated as a bar graph representing Mean ± SD. Statistical significance is measured by Student's t test where **** $p < 0.001$, and *** $p< 0.005$ for n=3.

(U) TBK1/Sec5/mTOR and PKR/Exo84/MST1 form protein complexes in sensitive cells. PKR and TBK1 was immunoprecipitated in the presence or absence of SeV from HCC44 (lung) and A375 (melanoma) cells and probed for coimmunoprecipitation for the indicated proteins.

Table S2, related to STAR methods and Figure 1: Exo84 interactome in the presence or absence of pI:C

Proteins	Average SC (-pI:C)	Average SC (+pI:C)
Exo84	21.5	23
EXOC7	4.5	4.5
EXOC6	3	3.5
EXOC5	3	3
Sec8	14	3
EIF2AK2	0.5	7.5
NKRF	2.5	5.5
EIF23E	6	0.5

***SC**= Spectral count

Table S3, related to STAR methods and Figure 1: Sec5 interactome in the presence or absence of pI:C

Proteins	Average SC (-pI:C)	Average SC (+pI:C)
Sec5	28	26
EXOC1	3.5	4.5
EXOC3	2.5	3.5
Sec8	4.5	6

*__SC__= Spectral count

Table S4, related to STAR methods and Figure 2: de-novo TBK1 interactome

Protein	Average SC (Flag-Empty)	Avergae SC (Flag-TBK1)	Average SC (Flag-TBK1-KD)	Log2 TBK1-endogenous (+pI:C/-pI:C)
CEP128	0	9.5		
IFIT1	0	10.0		
IFITM2	0	4.5		
ISG15	0	3.0		
RPS6KB1	0	3.0		
RPTOR	0	4.5		
TBK1	0	26.0	16.5	0
ATR	0	4.0	2.5	0
DDRGK1				0
HERC2				-2.5
NUBP2				0
Sec5	0	2.0		2
Sec8	0	2.5		2.5
TOR1AIP1				-1
WASH6P				-0.5
BRE				-1
YAP1	0	2.0	2.5	
TGFBI	0	1.0	4.5	
YWHAE	0	0.0	2.5	

***SC**= Spectral count

Table S5, related to STAR methods and Figure 2: Endogenous PKR partners and their enrichment or depletion upon presence or absence of pI:C stimuli

Protein	Log2 [{Average SC (+pI:C)}/{Average SC(-pI:C)}]
Exo84	6
WDR82	0.5
PTPN1	0
Sec5	0
EIF2A	0
KIBRA	0
MST1	0
CSNK2A2	0
PRKRA	0
NF2	0
PVR	0
NT5DC1	0
TBCD	0
ACOT9	0
PKR	-0.5
DDRGK1	-1

*__SC__= Spectral count

Table S6, related to STAR methods, Figure 6 and Figure S 6: RALB interactome

Proteins	SC (Replicate1)	SC (Replicate2)	SC (Replicate3)	SC (Replicate4)	SC (IgG control)
AMOTL1	2.0	2.0	5.0	1.0	0.00
ARPC1B	18.0	13.0	13.0	14.0	0.00
ARPC5	7.0	4.0	7.0	6.0	0.00
ARPC5L	4.0	3.0	4.0	4.0	0.00
ATP6V0D1	5.0	7.0	9.0	8.0	0.00
ATP6V1C1	3.0	2.0	3.0	2.0	0.00
CHUK	2.0	2.0	2.0	2.0	0.00
EXOC2	3.0	3.0	3.0	3.0	0.00
EXOC6	2.0	2.0	2.0	2.0	0.00
KIAA0196	2.0	3.0	4.0	3.0	0.00
LAMTOR1	6.0	5.0	6.0	7.0	0.00
LAMTOR3	2.0	2.0	3.0	1.0	0.00
MTOR	4.0	6.0	3.0	4.0	0.00
NF2	2.0	2.0	8.9	2.0	0.00
RAGA	2.0	2.0	2.0	2.0	0.00
RAGD	2.0	2.0	2.0	2.0	0.00
RALB	15.0	13.0	11.0	18.0	0.00
ROCK2	2.0	4.0	3.0	1.0	0.00
STK4	2.0	2.0	2.0	2.0	0.00
VPS4A	2.5	2.0	3.5	2.5	0.00
YAP1	2.0	2.0	9.0	2.0	0.00

*__SC__= Spectral count

Table S7, related to STAR methods, Figure 6 and Figure S 6: RALB dependent Exo84 and Sec5 interactome *(visual network representation of the table is below)*

Protein name	Average SC (RALB+Exo84)	Average SC (RALB+Sec5)	{Average SC (RALB+Exo84)} / {Average SC (RALB+Sec5)}	Log_2 [{Average SC (RALB+Exo84)} / {Average SC (RALB+Sec5)}]
Exo84	44	1	44	5.46
RIOK1	6	0.5	12	3.58
PRPSAP1	9	1	9	3.17
MST1	8	1	8	3.00
EIF3X	3.5	0.5	7	2.81
EIF2AK2	6	1	6	2.58
DENR	3	0.5	6	2.58
AP3S1	3	0.5	6	2.58
VPS4B	3	0.5	6	2.58
ULK1	5	1	5	2.32
RPTOR	5	1	5	2.32
EXOC7	2.5	0.5	5	2.32
LAMTOR2	4	1	4	2.00
LAMTOR3	2	0.5	4	2.00
LAMTOR1	5	2	2.5	1.32
EXOC6	2.5	1	2.5	1.32
EXOC5	1.5	3	0.5	-1.00
EXOC1	1.5	3.5	0.429	-1.22
VAPA	5	15	0.333	-1.58
mTOR	0.5	2	0.25	-2.00
METAP2	1	4.93	0.203	-2.30
Sec5	1	5.99	0.167	-2.58
METAP1	0.5	3	0.167	-2.58
MAP2K1	1	8	0.125	-3.00
COPS2	0.5	4.5	0.111	-3.17

Sec8	1	9.97	0.1	-3.32
MRTO4	1.5	16	0.094	-3.42
GTF2EF2	1	12	0.083	-3.58
EXOC3	1	18	0.056	-4.17

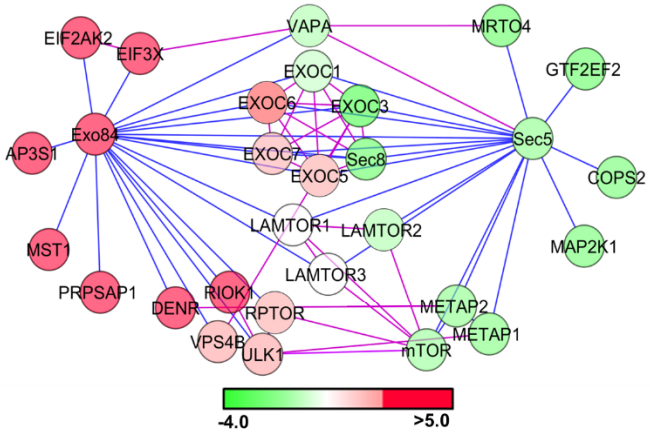

RALB+Sec5 RALB+Exo84

*Legends for the node and edges as described in Figure legends 1D.